

Measurement of Magic Wavelengths for the $^{40}\text{Ca}^+$ Clock Transition

Pei-Liang Liu,^{1,2,3} Yao Huang,^{1,2} Wu Bian,^{1,2,3} Hu Shao,^{1,2,3} Hua Guan,^{1,2,†} Yong-Bo Tang,^{1,4,§}
Cheng-Bin Li,^{1,2} J. Mitroy,^{5,*} and Ke-Lin Gao^{1,2,‡}

¹State Key Laboratory of Magnetic Resonance and Atomic and Molecular Physics,
Wuhan Institute of Physics and Mathematics, Chinese Academy of Sciences, Wuhan 430071, China

²Key Laboratory of Atomic Frequency Standards, Wuhan Institute of Physics and Mathematics,
Chinese Academy of Sciences, Wuhan 430071, China

³University of Chinese Academy of Sciences, Beijing 100049, China

⁴Department of Physics, Wuhan University, Wuhan 430072, China

⁵School of Engineering, Charles Darwin University, Darwin, Northern Territory 0909, Australia

(Received 8 September 2014; revised manuscript received 27 February 2015; published 2 June 2015)

We demonstrate experimentally the existence of magic wavelengths and determine the ratio of oscillator strengths for a single trapped ion. For the first time, two magic wavelengths near 396 nm for the $^{40}\text{Ca}^+$ clock transition are measured simultaneously with high precision. By tuning the applied laser to an intermediate wavelength between transitions $4s_{1/2} \rightarrow 4p_{1/2}$ and $4s_{1/2} \rightarrow 4p_{3/2}$, the sensitivity of the clock transition Stark shift to the oscillator strengths is greatly enhanced. Furthermore, with the measured magic wavelengths, we determine the ratio of the oscillator strengths with a deviation of less than 0.5%. Our experimental method may be applied to measure magic wavelengths for other ion clock transitions. Promisingly, the measurement of these magic wavelengths paves the way to building all-optical trapped ion clocks.

DOI: 10.1103/PhysRevLett.114.223001

PACS numbers: 31.15.ac, 31.15.ap, 34.20.Cf

The magic wavelength for an atomic transition is a wavelength for which the ac Stark shift vanishes [1–5]. The existence of magic wavelength enables independent control of internal hyperfine-spin and external center-of-mass motions of atoms (including neutral atoms and atomic ions). Precision measurements of magic wavelengths in atoms are very important in studies of atomic structure. For example, a measurement of the line strength ratio can bring a new perspective for determining accurate transition matrix elements, which are important in testing atomic structure theories, as well as the reliability of a model used in interpreting atomic parity nonconservation [6–8]. The oscillator strength, which is directly related to the line strength and is critical in astrophysical data analysis [9], can be derived from the magic wavelengths. Furthermore, the knowledge of oscillator strengths and polarizabilities for clock states is essential to correct the blackbody radiation shift. In addition, a similar concept is the tune-out wavelength [10], at which the dynamic polarizability of the concerned atomic state is zero. Recently, by measuring the tune-out wavelengths, the line strength ratios have been derived for neutral potassium and rubidium [11,12].

Until now, magic wavelengths have provided extensive applications in quantum state engineering and precision frequency metrology [2]. Magic wavelengths in neutral atomic systems have been measured in several experiments [4,13–16]. The optical dipole trap at the magic wavelength can eliminate the first-order Stark shift and so that the systematic uncertainties can be reduced. Atomic clocks based on neutral atoms trapped in the magic wavelength optical lattices are a new trend of development for optical

clocks [1,17–19]. Recently, all-optical trapping of ions has been demonstrated [20,21] and it is important to explore the possibility of trapping ions via magic wavelength lasers. With the all-optical trapping technique, an ion clock can be built with better performance. Therefore, the demonstration of magic wavelengths for ion clock transitions is a milestone for establishing all-optical trapped ion clocks.

In this Letter, for the first time, two magic wavelengths for the $^{40}\text{Ca}^+$ clock transition are reported and a novel application of magic wavelengths in determining the oscillator strength ratio is presented. As the $^{40}\text{Ca}^+$ optical clock is a typical ion optical clock, our method for measuring magic wavelengths can be applied to other similar systems, such as Sr^+ , In^+ , Hg^+ , Al^+ , and Ba^+ , which have been chosen as candidates for building optical clocks [22–27].

In Fig. 1, we show the involved energy levels of $^{40}\text{Ca}^+$. In our experiment, we apply a laser to induce an ac Stark shift to the $^{40}\text{Ca}^+ 4s_{1/2} \rightarrow 3d_{5/2}$ ion clock transition for the

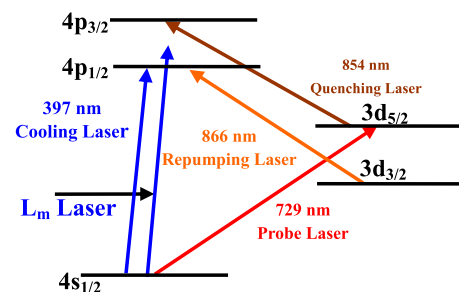


FIG. 1 (color online). Partial energy level diagram of $^{40}\text{Ca}^+$.

$|m_j| = 1/2$ and $|m_j| = 3/2$ magnetic sublevels of the $3d_{5/2}$ state. The magic wavelengths are determined by measuring the ac Stark shifts for different laser frequencies. There are two magic wavelengths, $\lambda_{m_j=+1/2}$ and $\lambda_{m_j=-1/2}$, corresponding to the magnetic substates $m_j = \pm 1/2$ of the $3d_{5/2}$ level. The magic wavelength $\lambda_{|m_j|}$ is the average of λ_{+m_j} and λ_{-m_j} , with $m_j = \{1/2, 3/2\}$. The measured magic wavelengths near 396 nm lie between the resonant $4s_{1/2} \rightarrow 4p_{1/2}$ and $4s_{1/2} \rightarrow 4p_{3/2}$ transitions; see Fig. 1. Theoretical calculations indicate that these magic wavelengths are very sensitive to the ratio of the $4s_{1/2} \rightarrow 4p_{3/2}$ to $4s_{1/2} \rightarrow 4p_{1/2}$ oscillator strengths [28]. The $^{40}\text{Ca}^+$ resonant oscillator strength cannot be determined with a single measurement since the $4p_J$ states can decay to either the $4s_{1/2}$ ground state or the $3d_J$ excited states. Besides the $4p_J$ lifetimes, one also needs the branching ratio for the transitions to the $4s_{1/2}$ and $3d_J$ states [29–32] since the $4p_J \rightarrow 3d_J$ transitions make a contribution of about 6% to the lifetimes [28,32,33]. One of the advantages of the magic wavelength approach is that the contribution to the polarizability from the $4s_{1/2} \rightarrow 4p_J$ transitions at the magic wavelength is 3 orders of magnitude larger than the contribution from other transitions.

For an ion in a single-mode laser field, the energy shift of a given atomic state a can be written as [14]

$$\Delta E_a = -\alpha_a(\omega)I - \beta_a(\omega)I^2 + O(I^3), \quad (1)$$

where $\alpha_a(\omega)$ and $\beta_a(\omega)$ are the dynamic dipole polarizability and hyperpolarizability, respectively. Here, I is the laser intensity and $O(I^3)$ represents the residual high-order Stark shift. For the $^{40}\text{Ca}^+$ optical clock, one of major experimental concerns is the frequency shift of the clock transition caused by electromagnetic radiation, which can be written as

$$\begin{aligned} h\Delta\nu &= \Delta E_d(\omega) - \Delta E_s(\omega) \\ &= -\Delta\alpha(\omega)I - \Delta\beta(\omega)I^2 + \Delta O(I^3), \end{aligned} \quad (2)$$

where $\Delta\alpha(\omega)$ and $\Delta\beta(\omega)$ are the differential dipole polarizability and hyperpolarizability, respectively. At the magic wavelength $\lambda_{m_j} = c/\omega_{m_j}$ (where c is the speed of light in vacuum), the frequency shift $\Delta\nu = 0$. Under the weak intensity limit, the frequency shifts contributed by the hyperpolarizability and the residual higher-order terms are several orders of magnitude smaller than the linear term $\Delta\alpha(\omega)I$. This means that, by neglecting all nonlinear Stark shifts, the magic wavelength λ_{m_j} can be theoretically given by the condition $\Delta\alpha(\omega) = 0$. Using current available techniques for the ion optical clock, the differential light shift $\Delta\nu$ can be measured accurately, and therefore the magic wavelength can be determined with high precision.

Our experimental setup for measuring magic wavelengths is shown in Fig. 2. The whole system includes two main parts: (i) the optical clock based on single trapped

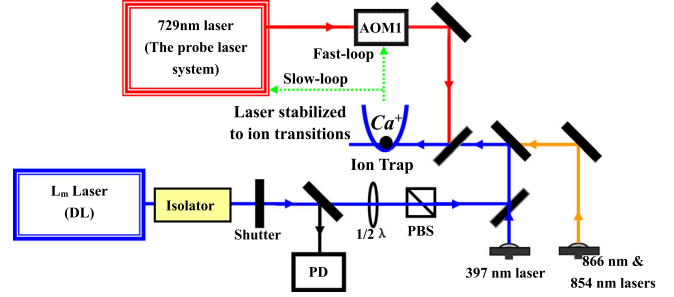


FIG. 2 (color online). Schematic diagram of the magic wavelength measurement setup. DL: diode laser; AOM: acousto-optic modulator; $1/2\lambda$: half wave plate; PD: photo diode; PBS: polarized beam splitter.

$^{40}\text{Ca}^+$ and (ii) the L_m laser system for measuring the frequency shift of the clock transition.

The details of the ion optical clock has been described in our previous work [34,35]. A 729 nm probe laser is locked to an ultrastable, high finesse cavity mounted on a vibration isolation platform (TS-140) by the Pound-Drever-Hall method, and an acousto-optic modulator is used to cancel the slow linear drift of the reference cavity.

The frequency of our L_m laser is stabilized by using a transfer cavity referenced to the 729 nm probe laser. The long-term drift of our L_m laser is reduced to less than 10 MHz within four hours. An unpolarized beam splitter is used to split a part of light for monitoring the laser power, which is $700 \mu\text{W}$ with a jitter of $3 \mu\text{W}$. The power meter used in the experiment is a commercial power meter (S120VC, Thorlabs, Inc.). The powers of the incident and output beams of the L_m laser are monitored simultaneously. The power of the L_m laser into the trap is $731(4) \mu\text{W}$ and the waist radius of the beam is $203(5) \mu\text{m}$ during the measurement. A polarized beam splitter is placed in the light path before the ion-light interaction maintains the linear polarization of the L_m laser. In this way, the linear polarization purity can reach 99.9%, which can be derived by analyzing the polarization of the incident light and the transmission light of the L_m laser.

In our experiment, a single $^{40}\text{Ca}^+$ ion is trapped in a miniature Paul trap and then cooled to a few mK. The excess micromotion of the ion is minimized by adjusting the voltages of two compensation electrodes and two end-cap electrodes with the rf-photon correlation technique [36] before performing any measurements. The s - d clock transition splits symmetrically into ten Zeeman components around the zero-field line center [35]. Then the probe laser is further referenced to the $^{40}\text{Ca}^+$ ion clock transitions by feeding back to the frequency of the acousto-optic modulator (AOM1) to compensate for changes in the magnetic field and to probe the individual Zeeman transitions. The pulse sequences of 397, 866, 854, and 729 nm lasers are similar to that used in the $^{40}\text{Ca}^+$ ion optical frequency standard [35]. The pulse sequence of the L_m

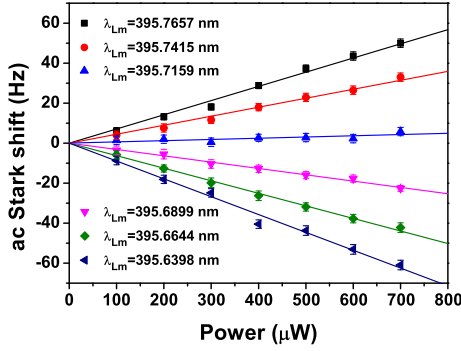


FIG. 3 (color online). The ac Stark shift versus the incident L_m laser power for different laser wavelengths. All measurements correspond to the $^{40}\text{Ca}^+$ ion clock transition $4s_{1/2} \rightarrow 3d_{5/2}$ for the $m_j = +1/2$ magnetic sublevel of the $3d_{5/2}$ state.

laser is introduced to measure the light shift. The L_m laser is switched off during the Doppler cooling period, and it is switched on and off alternately during the probing stage to measure the light shift. The frequency values of AOM1 are recorded automatically every cycle by a personal computer and the light shift caused by the L_m laser beam can be measured by calculating the difference between two on-off cycles with the L_m laser.

By using techniques for the ion optical clock, we measure the ac Stark shifts around the magic wavelength λ_{m_j} . We choose six fixed wavelengths of the L_m laser and measure the ac Stark shifts for each wavelength by switching the L_m laser on and off. In order to show the relation between the incident laser power and the ac Stark shift, we measure the ac Stark shifts of the $^{40}\text{Ca}^+$ ion clock transition $4s_{1/2} \rightarrow 3d_{5/2}$ for the $m_j = +1/2$ magnetic sublevel of the $3d_{5/2}$ state at different powers; see Fig. 3. Our experimental data show a linear dependence between the ac Stark shift and the incident laser power, which indicates that the nonlinear terms in Eq. (2) can be neglected. Because of the laser beam direction may change slightly, the incident power of the L_m laser shining on the ion may also changes slightly when tuning the wavelength. Therefore the power is calibrated to ensure that it is identical within 4% at all six wavelengths. To obtain the magic wavelength, we fit a linear function to the measured ac Stark shifts for the same incident power and different laser wavelengths. In Fig. 4, for the same incident power, $700 \mu\text{W}$, we show the ac Stark shift versus the laser wavelength.

Because of the influence of the uncertainties from the wave-meter measurement, the broadband spectral component and the power jitter of the L_m laser, it is difficult to obtain the frequency difference by separate measurements of $|m_j| = 1/2$ and $|m_j| = 3/2$. Here a new measurement protocol has been adopted. In our experiment, for each of the six L_m laser wavelengths, we measure the ac Stark shifts for, respectively, $|m_j| = 1/2$ and $|m_j| = 3/2$ of the $3d_{5/2}$ state. This procedure is repeated until the ac Stark shifts for all six L_m laser wavelengths have been measured.

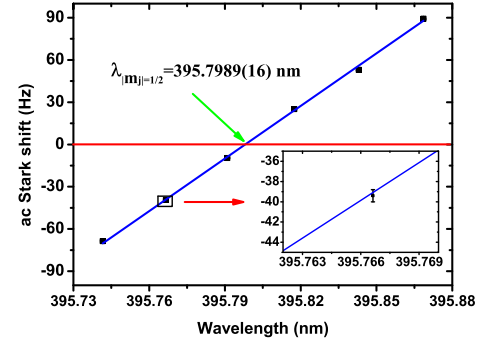


FIG. 4 (color online). The ac Stark shift versus the laser wavelength. The power of the L_m laser is fixed at $700 \mu\text{W}$. Each data point represents 2000 s of experimental data. The blue solid line is the linear fit to the data. The zero ac Stark shift wavelength is identified as λ_{m_j} . The inset shows the magnification for one measurement point.

The L_m laser wavelength is tuned from 395.7 to 395.9 nm, then from 395.9 to 395.7 nm. In Fig. 5, we show ten measurements for $\lambda_{|m_j|=1/2}$ and $\lambda_{|m_j|=3/2}$, respectively. The corresponding weighted means give $\lambda_{|m_j|=1/2} = 395.7992(2) \text{ nm}$ and $\lambda_{|m_j|=3/2} = 395.7990(2) \text{ nm}$. The difference between $\lambda_{|m_j|=1/2}$ and $\lambda_{|m_j|=3/2}$ is $0.0002(6) \text{ nm}$, which agrees with the theoretical calculation [28].

To give the final magic wavelengths, one has to take into account the systematic shifts and their corresponding corrections to the above averaged frequencies. The systematic shifts may be caused by the broad spectral component, the light polarization, the second-order Doppler shift, the calibration of the wave meter, etc. The error budget is given in Table I.

One major error of the magic wavelength measurement comes from the broad spectral component of L_m . To estimate the broad spectral component, a grating spectrometer (IHR550, HORIBA) has been used to analyze the laser spectrum. We find that more than 99% of the laser power is

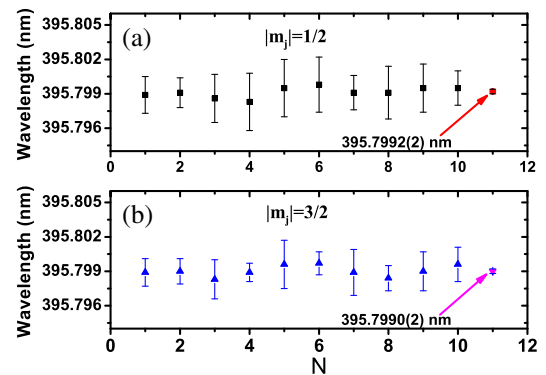


FIG. 5 (color online). (a) The ten measurements (the black squares) of $\lambda_{|m_j|=1/2}$. (b) The ten measurements (the blue triangles) of $\lambda_{|m_j|=3/2}$. The solid red circles and the solid purple triangles stand for the weighted means. The error bars show the statistical errors of the ten measurements.

TABLE I. The uncertainty budget of the magic wavelength measurement.

| Sources of uncertainty | Shift (pm) | Uncertainty (pm) |
|---------------------------------------|------------|------------------|
| Broadband light | 0 | 0.60 |
| Light polarization | 0 | 0.01 |
| Second-order Doppler and Stark shifts | 0.01 | 0.01 |
| Laser wavelength | 0 | 0.06 |
| Statistical uncertainty | ... | 0.20 |
| Total | 0.01 | 0.7 |

within the wavelength range of 0.03 nm and only less than 1% laser power is out of that range, which corresponds to a less than 0.0005 nm contribution to the uncertainty in $\lambda_{|m_j|=1/2}$ and $\lambda_{|m_j|=3/2}$ [12]. Next, the spectral component in the range of 0.03 nm around the carrier is analyzed by observing the beat note of the L_m lasers with another similar laser by using a spectrum analyzer. The spectrum contains three main components from which the ac Stark shift could be estimated based on their relative weights, and only an uncertainty of less than 0.0001 nm is obtained. Lights with different polarizations can result in different ac Stark shifts. Elliptical polarization will have scalar, vector, and tensor light shifts for atoms with $|m_F| > 0$ [37], which will change the value of the magic wavelength. In our experiment, a polarized beam splitter (PBS) has been used to create a pure linear polarization, and the ellipticity component is reduced to less than 0.1% by analyzing the light beam before and after the vacuum chamber. To estimate the contribution due to the nonlinearly polarized component, the uncertainty with circularly polarized light is measured and the wavelength difference with linearly and circularly polarized light is less than 0.01 nm; thus, there would only be less than 0.0001 nm of uncertainty with less than 0.1% ellipticity.

The L_m laser may heat the ion and affect the cooling efficiency; therefore, a second order Doppler shift and a Stark shift may appear due to the increase of the ion temperature or the ion micromotion. To estimate the second-order Doppler shift, the ion temperature is measured by monitoring the intensity of secular sidebands and the ion micromotion is measured by using the rf-photon correlation method [36] with and without the L_m laser. Our data show that the ion temperature and the ion micromotion result in an uncertainty of 0.00001 nm. The L_m laser wavelength after frequency stabilization is monitored by a wave meter (High Finesse WS-7) with an absolute accuracy of 60 MHz after the calibration by using the clock laser. The uncertainty from the calibration of the wave meter is within 0.00006 nm. Taking into account the above effects, the magic wavelengths are given as 395.7992(7) and 395.7990(7) nm, which locate in the spin-orbit energy gap of the $4p$ state.

The ac Stark shift is strongly dominated by the large and opposite polarizability contributions from the $4p_{1/2}$ and $4p_{3/2}$ states [11,28,38]. The contributions of the $3d_{5/2}$

polarizabilities are typically small in magnitude at the magic wavelengths near 396 nm. Thus, for the weak laser intensity in our experiment, by neglecting all nonlinear Stark shifts, the difference of the dynamic dipole polarizabilities at the magic wavelength can be written as

$$0 = \alpha_{4s_{1/2}}(\omega_{m_j}) - \alpha_{3d_{5/2}}(\omega_{m_j}) \\ \cong \frac{f(4s_{1/2} \rightarrow 4p_{1/2})}{\epsilon_{4s_{1/2} \rightarrow 4p_{1/2}}^2 - \omega_{m_j}^2} + \frac{f(4s_{1/2} \rightarrow 4p_{3/2})}{\epsilon_{4s_{1/2} \rightarrow 4p_{3/2}}^2 - \omega_{m_j}^2} + \Delta, \quad (3)$$

with the transition energy ϵ and the oscillator strength f . Here, Δ consists of the residual terms in the $4s_{1/2}$ polarizability as well as the small $3d_{5/2}$ polarizabilities, which are estimated to be $2.95a_0^3$ for the $3d_{m_j=1/2}$ state and $0.31a_0^3$ for the $3d_{m_j=3/2}$ state. The value of $f(4s_{1/2} \rightarrow 4p_{1/2}) = 0.3171$ is given by our theoretical calculation.

Based upon the energies of the $4s_{1/2}$, $4p_{1/2}$, and $4p_{3/2}$ states given by the NIST Database [39] and the magic wavelengths λ_{m_j} measured by us, from Eq. (3), we obtain the oscillator strength ratio

$$R_f = \frac{f(4s_{1/2} - 4p_{3/2})}{f(4s_{1/2} - 4p_{1/2})} = 2.027(5), \quad (4)$$

and the line strength ratio

$$R_s = \frac{|\langle 4s \| D \| 4p_{3/2} \rangle|^2}{|\langle 4s \| D \| 4p_{1/2} \rangle|^2} = 2.009(5). \quad (5)$$

A change in Δ by $2.0a_0^3$ will result in a change in the derived R_s by 0.001. Changes in the oscillator strengths of the background transitions of more than 5% would be needed to change Δ by $2.0a_0^3$ and the uncertainty estimates in R_s and R_f allows for this. The previously estimated line strength ratios of 2.001 [33] and 2.0014 [28] were based on the relativistic all-order many-body perturbation theory and the relativistic semiempirical potential, respectively. Since the results for $\omega_{m_j=1/2}$ and $\omega_{m_j=3/2}$ are very close to each other, taking into account both experimental and theoretical uncertainties, the oscillator strength ratio and the line strength ratio ratios are given as $R_f = 2.027(5)$ and $R_s = 2.009(5)$.

In summary, two magic wavelengths of $\lambda_{|m_j|=1/2} = 395.7992(7)$ nm and $\lambda_{|m_j|=3/2} = 395.7990(7)$ nm of the $^{40}\text{Ca}^+$ clock transition have been measured within an accuracy of 2 ppm. Our experiment is the first demonstration of magic wavelengths in an ion optical clock system. The oscillator strength ratio and the line strength ratio for the transitions $f(4s_{1/2} \rightarrow 4p_{3/2,1/2})$ have been determined to be 2.027(5) and 2.009(5). At present, the broadband spectrum of the L_m laser and statistical error were the largest contributors to the total systematic uncertainty. These errors can be reduced by introducing a cavity for mode selection to the L_m laser and by improving the

power stabilization, respectively. An order of magnitude improvement over the currently determined magic wavelengths will therefore be achievable in future work.

We thank Ting-Yun Shi and Li-Yan Tang for their valuable suggestions. We also thank Z.-C. Yan (University of New Brunswick, Canada), J. Ye (JILA), H. Klein (National Physical Laboratory, United Kingdom), C. Lee (Sun Yat-Sen University, Guangzhou, China), X. Guan, J. Chen (Institute of Applied Physics and Computational Mathematics, Beijing, China), and R. A. Roemer (University of Warwick) for the fruitful discussions. Thank you to X. Huang, H. Shu, H. Fan, B. Guo, Q. Liu, W. Qu, J. Cao, and B. Ou for the early experiments. This work is supported by the National Basic Research Program of China (Grant No. 2012CB821301), the National Natural Science Foundation of China (Grants No. 11474318, No. 91336211, and No. 11034009), and the Chinese Academy of Sciences.

*Deceased.

†Corresponding author.

guanhua@wipm.ac.cn

‡Corresponding author.

klgao@wipm.ac.cn

§Present address: Department of Physics, Henan Normal University, Xinxiang 453007, China.

- [1] M. Takamoto, F.-L. Hong, R. Higashi, and H. Katori, *Nature (London)* **435**, 321 (2005).
- [2] J. Ye, H. J. Kimble, and H. Katori, *Science* **320**, 1734 (2008).
- [3] Z. W. Barber, J. E. Stalnaker, N. D. Lemke, N. Poli, C. W. Oates, T. M. Fortier, S. A. Diddams, L. Hollberg, C. W. Hoyt, A. V. Taichenachev, and V. I. Yudin, *Phys. Rev. Lett.* **100**, 103002 (2008).
- [4] L. Yi, S. Mejri, J. J. McFerran, Y. Le Coq, and S. Bize, *Phys. Rev. Lett.* **106**, 073005 (2011).
- [5] J. Mitroy, M. S. Safronova, and C. W. Clark, *J. Phys. B* **43**, 202001 (2010).
- [6] A. Derevianko, *Phys. Rev. Lett.* **85**, 1618 (2000).
- [7] B. K. Sahoo, R. Chaudhuri, B. P. Das, and D. Mukherjee, *Phys. Rev. Lett.* **96**, 163003 (2006).
- [8] S. G. Porsev, K. Beloy, and A. Derevianko, *Phys. Rev. Lett.* **102**, 181601 (2009).
- [9] R. L. Kurucz, *Can. J. Phys.* **89**, 417 (2011).
- [10] L. J. LeBlanc and J. H. Thywissen, *Phys. Rev. A* **75**, 053612 (2007).
- [11] C. D. Herold, V. D. Vaidya, X. Li, S. L. Rolston, J. V. Porto, and M. S. Safronova, *Phys. Rev. Lett.* **109**, 243003 (2012).
- [12] W. F. Holmgren, R. Trubko, I. Hromada, and A. D. Cronin, *Phys. Rev. Lett.* **109**, 243004 (2012).
- [13] A. Brusch, R. Le Targat, X. Baillard, M. Fouché, and P. Lemonde, *Phys. Rev. Lett.* **96**, 103003 (2006).
- [14] M. Takamoto, H. Katori, S. I. Marmo, V. D. Ovsiannikov, and V. G. Pal'chikov, *Phys. Rev. Lett.* **102**, 063002 (2009).
- [15] N. D. Lemke, A. D. Ludlow, Z. W. Barber, T. M. Fortier, S. A. Diddams, Y. Jiang, S. R. Jefferts, T. P. Heavner, T. E. Parker, and C. W. Oates, *Phys. Rev. Lett.* **103**, 063001 (2009).
- [16] A. D. Ludlow, T. Zelevinsky, G. K. Campbell, S. Blatt, M. M. Boyd, M. H. G. de Miranda, M. J. Martin, J. W. Thomsen, S. M. Foreman, J. Ye, T. M. Fortier, J. E. Stalnaker, S. A. Diddams, Y. Le Coq, Z. W. Barber, N. Poli, N. D. Lemke, K. M. Beck, and C. W. Oates, *Science* **319**, 1805 (2008).
- [17] B. J. Bloom, T. L. Nicholson, J. R. Williams, S. L. Campbell, M. Bishof, X. Zhang, W. Zhang, S. L. Bromley, and J. Ye, *Nature (London)* **506**, 71 (2014).
- [18] H. S. Margolis, *J. Phys. B* **42**, 154017 (2009).
- [19] N. Hinkley, J. A. Sherman, N. B. Phillips, M. Schioppo, N. D. Lemke, K. Beloy, M. Pizzocaro, C. W. Oates, and A. D. Ludlow, *Science* **341**, 1215 (2013).
- [20] I. V. Krasnov and L. P. Kamenshchikov, *Opt. Commun.* **312**, 192 (2014).
- [21] M. Enderlein, T. Huber, C. Schneider, and T. Schaetz, *Phys. Rev. Lett.* **109**, 233004 (2012).
- [22] P. Dubé, A. A. Madej, M. Tibbo, and J. E. Bernard, *Phys. Rev. Lett.* **112**, 173002 (2014).
- [23] G. P. Barwood, G. Huang, H. A. Klein, L. A. M. Johnson, S. A. King, H. S. Margolis, K. Szymaniec, and P. Gill, *Phys. Rev. A* **89**, 050501 (2014).
- [24] K. Hayasaka, *Appl. Phys. B* **107**, 965 (2012).
- [25] Y. H. Wang, R. Dumke, T. Liu, A. Stejskal, Y. N. Zhao, J. Zhang, Z. H. Lu, L. J. Wang, T. Becker, and H. Walther, *Opt. Commun.* **273**, 526 (2007).
- [26] T. Rosenband, D. B. Hume, P. O. Schmidt, C. W. Chou, A. Brusch, L. Lorini, W. H. Oskay, R. E. Drullinger, T. M. Fortier, J. E. Stalnaker, S. A. Diddams, W. C. Swann, N. R. Newbury, W. M. Itano, D. J. Wineland, and J. C. Bergquist, *Science* **319**, 1808 (2008).
- [27] A. Kleczewski, M. R. Hoffman, J. A. Sherman, E. Magnuson, B. B. Blinov, and E. N. Fortson, *Phys. Rev. A* **85**, 043418 (2012).
- [28] Y.-B. Tang, H.-X. Qiao, T.-Y. Shi, and J. Mitroy, *Phys. Rev. A* **87**, 042517 (2013).
- [29] A. Gallagher, *Phys. Rev.* **157**, 24 (1967).
- [30] R. N. Gosselin, E. H. Pinnington, and W. Ansbacher, *Phys. Rev. A* **38**, 4887 (1988).
- [31] J. Jin and D. A. Church, *Phys. Rev. Lett.* **70**, 3213 (1993).
- [32] R. Gerritsma, G. Kirchmair, F. Zähringer, J. Benhelm, R. Blatt, and C. F. Roos, *Eur. Phys. J. D* **50**, 13 (2008).
- [33] M. S. Safronova and U. I. Safronova, *Phys. Rev. A* **83**, 012503 (2011).
- [34] Y. Huang, Q. Liu, J. Cao, B. Ou, P. Liu, H. Guan, X. Huang, and K. Gao, *Phys. Rev. A* **84**, 053841 (2011).
- [35] Y. Huang, J. Cao, P. Liu, K. Liang, B. Ou, H. Guan, X. Huang, T. Li, and K. Gao, *Phys. Rev. A* **85**, 030503 (2012).
- [36] D. J. Berkeland, J. D. Miller, J. C. Bergquist, W. M. Itano, and D. J. Wineland, *J. Appl. Phys.* **83**, 5025 (1998).
- [37] I. H. Deutsch and P. S. Jessen, *Opt. Commun.* **283**, 681 (2010).
- [38] B. Arora, M. S. Safronova, and C. W. Clark, *Phys. Rev. A* **76**, 052509 (2007).
- [39] A. Kramida, Y. Ralchenko, J. Reader, and NIST ASD Team, NIST Atomic Spectra Database (version 5.2), <http://physics.nist.gov/asd>.